

CHAOS VERSUS ORDER IN HAMILTONIAN DYNAMICAL SYSTEMS

G.R.W. QUISPEL *

*Department of Mathematics, LaTrobe University,
Bundoora, Victoria 3088, Australia*

ABSTRACT

These lectures give an introduction to the concepts of ordered and chaotic motion and the occurrence of these two types of motion in Hamiltonian dynamical systems. We illustrate the basic ideas and results using area-preserving mappings of the plane and consider an application of these ideas and techniques in a model of the solar system.

1. Introduction

1.1 Preamble

Motion can be broadly classified as belonging to one of two types: chaotic and ordered. Some systems have *only* chaotic motion while others exhibit *only* ordered motion. These represent two extreme possibilities. The phase space of most systems, however, contains both "ordered regions" and "chaotic regions". Whether a given orbit is ordered or chaotic will depend on whether it (or equivalently its initial conditions) lie in an ordered region or a chaotic region of phase space. We define more precisely what we mean by these terms below, however for now it will suffice to motivate these ideas with some pictures. Figures 1 to 3 depict the completely ordered, completely chaotic and both ordered and chaotic systems respectively. An explanation of the figures is required. In Figures 1 and 3 each closed curve corresponds to a single orbit, and a number of them are plotted. In contrast Figure 2 is a plot of just *one* orbit.

In these lectures we restrict ourselves to a treatment of Hamiltonian dynamical systems because of their relevance to statistical mechanics and their ubiquity in the modelling of physical systems. Hamiltonian systems, it will be shown, display the full range of motions depicted in Figures 1 to 3.

1.2 Hamiltonian Systems

A Hamiltonian system is one in which there exists a scalar function $H(q,p)$ (the Hamiltonian) satisfying

* Notes taken by G.S. Turner.

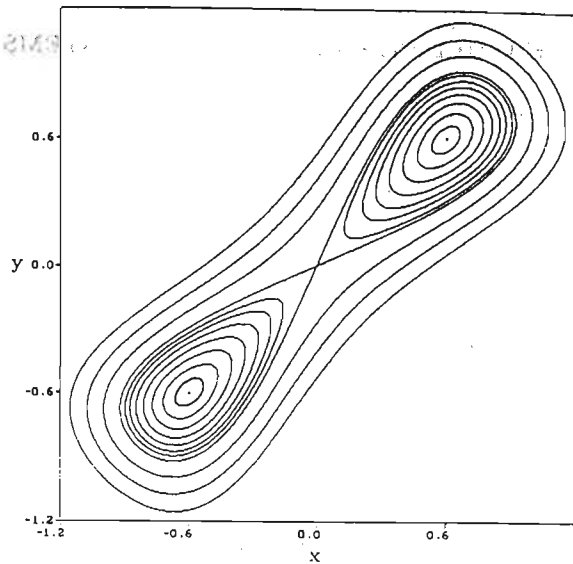


Figure 1: A system exhibiting complete order; described by the mapping $x' = y$, $y' = -x + 2ky/(1+y^2)$.

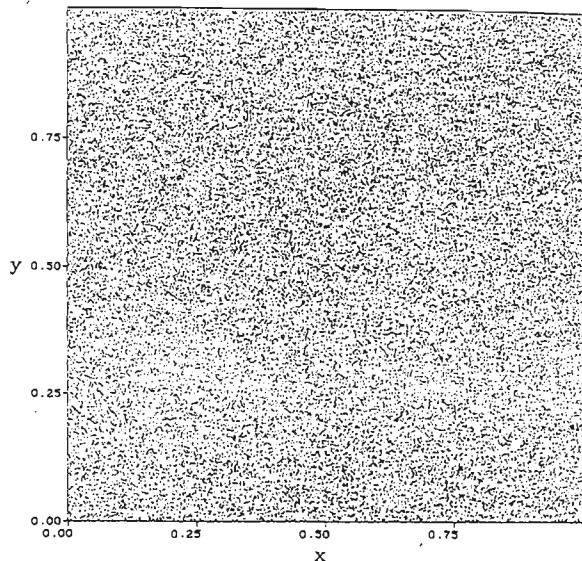


Figure 2: A system exhibiting complete chaos; described by the mapping $x' = x + y \pmod{1}$, $y' = x + 2y \pmod{1}$.

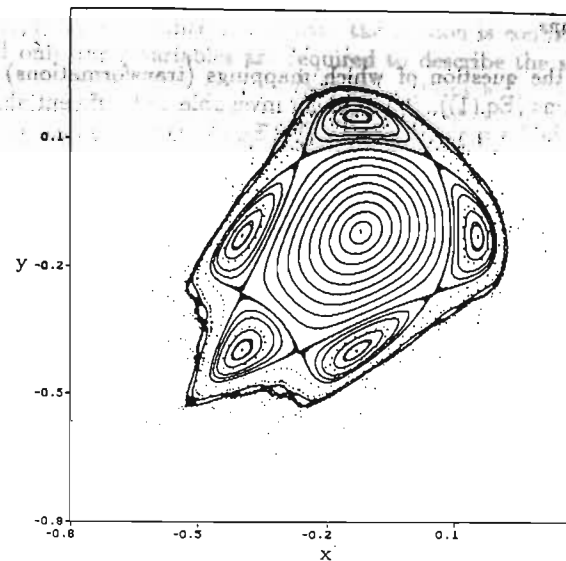


Figure 3: A system exhibiting a mixture of order and chaos; described by the mapping $x' = -y + 2(k-x^2)$, $y' = x$.

$$\begin{aligned} \frac{dq}{dt} &= \frac{\partial}{\partial p} H(\mathbf{q}, \mathbf{p}) \\ \frac{dp}{dt} &= -\frac{\partial}{\partial q} H(\mathbf{q}, \mathbf{p}) \end{aligned} \quad (1)$$

where $\mathbf{q} = (q_1, \dots, q_n)$ and $\mathbf{p} = (p_1, \dots, p_n)$ are the position and momentum vectors respectively*. Eq.(1) is a system of $2n$ ODE's with a special structure that is completely specified by a single function H . The Poisson bracket is defined as

$$\{F(\mathbf{q}, \mathbf{p}), G(\mathbf{q}, \mathbf{p})\} := \sum_{i=1}^n \left(\frac{\partial F}{\partial q_i} \frac{\partial G}{\partial p_i} - \frac{\partial F}{\partial p_i} \frac{\partial G}{\partial q_i} \right) \quad (2)$$

for arbitrary scalar functions F and G . Observe that Eq.(1) & (2) allow us to write the time-derivative of some dynamical quantity in terms of the Poisson bracket

$$\frac{dF(\mathbf{q}, \mathbf{p})}{dt} = \{F, H\} \quad (3)$$

* We restrict ourselves to autonomous Hamiltonian systems.

1.3 Symplectic Maps

We consider the question of which mappings (transformations) L preserve Hamilton's equations (Eq.(1)). Let L be an invertible and differentiable mapping. Combining the variables q and p as $z := \begin{pmatrix} q \\ p \end{pmatrix}$, Eq.(1) can be rewritten as

$$\frac{dz}{dt} = \omega \cdot \frac{\partial H}{\partial z} \quad (4)$$

where

$$\omega = \begin{pmatrix} 0 & Id \\ -Id & 0 \end{pmatrix} \quad (5)$$

We require the map $L : z \mapsto \hat{z}(z)$ (and $H(z) \mapsto \hat{H}(\hat{z})$) to be such that

$$\frac{d\hat{z}}{dt} = \omega \cdot \frac{\partial \hat{H}}{\partial \hat{z}} \quad (6)$$

from which it follows that L must satisfy

$$dL \cdot \omega \cdot dL^t = \omega \quad (7)$$

where dL is the Jacobian matrix of L . A map L satisfying Eq.(7) preserves Hamilton's equations and is called *symplectic*. Observe that by taking the determinant of both sides of Eq.(7) one obtains the condition $|\det(dL)| = 1$ which says that symplectic maps preserve volume. It can also be shown that symplectic maps form a group. Symplectic maps arise naturally in two ways:

1. **Flows** The flow of a Hamiltonian system is defined to be the (nonlinear) mapping φ_τ , which shifts orbits forward by time-interval τ , i.e.

$$\varphi_\tau : \begin{pmatrix} q(t) \\ p(t) \end{pmatrix} \mapsto \begin{pmatrix} q(t + \tau) \\ p(t + \tau) \end{pmatrix}$$

It is obvious that this equation leaves invariant Hamilton's equations (Eq.(1)). Hence Hamiltonian flows are symplectic.

2. **Poincaré Sections** Poincaré maps are obtained by constructing a surface or cross section (Σ) transverse to a Hamiltonian flow (Figure 4). Each time a trajectory crosses the surface (from below to above) a point is generated and the rule relating the points is called the Poincaré map (denoted P in Figure 4). Consider a Hamiltonian system of two degrees-of-freedom. The system is described by four

variables (q_1, q_2, p_1, p_2) . Since $H = \text{const.}$ the motion is confined to a 3D energy surface and only three variables are required to describe the system. By appropriately sectioning the 3D energy surface one obtains a further reduction in the dimension producing a 2D Poincaré map. It can be shown that the surface of section can be chosen such that the resulting map is symplectic. Because of the close relationship described above, we will discuss Hamiltonian systems of ODE's and symplectic maps interchangeably.

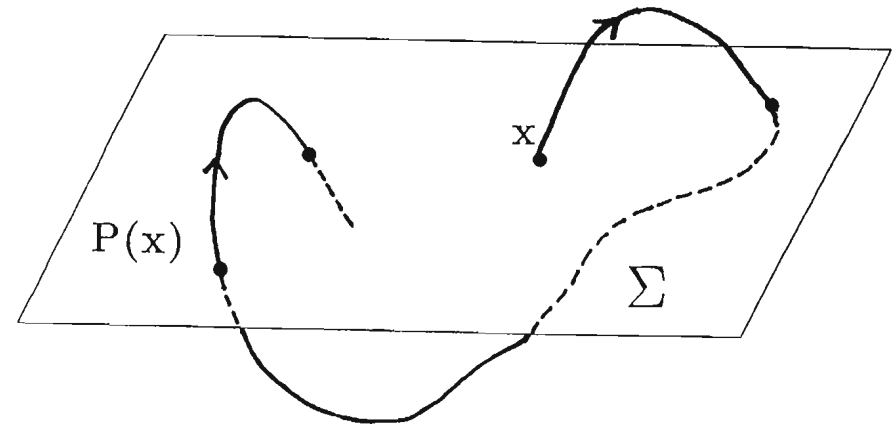


Figure 4: A Poincaré surface of section Σ and the associated Poincaré map $P, x \mapsto P(x)$.

2. Integrable Systems

2.1 Some Examples

Before we proceed to give a formal definition of integrability, we consider four examples of simple integrable Hamiltonian systems which exhibit different types of ordered motion.

Example 1: Free Particle

A one-dimensional particle moving in a zero potential has Hamiltonian

$$H(q, p) = \frac{1}{2}p^2 \quad (8)$$

and the equations of motion are thus

$$\frac{dq}{dt} = p, \quad \frac{dp}{dt} = 0 \quad (9)$$

Eq.(9) has solutions

$$p(t) = c, \quad q(t) = ct + q(0) \quad c \in \mathbf{R} \quad (10)$$

This example shows the first and simplest topological type of ordered motion: *unbounded uniform motion*. Particles move with constant speed c in straight lines (Figure 5).

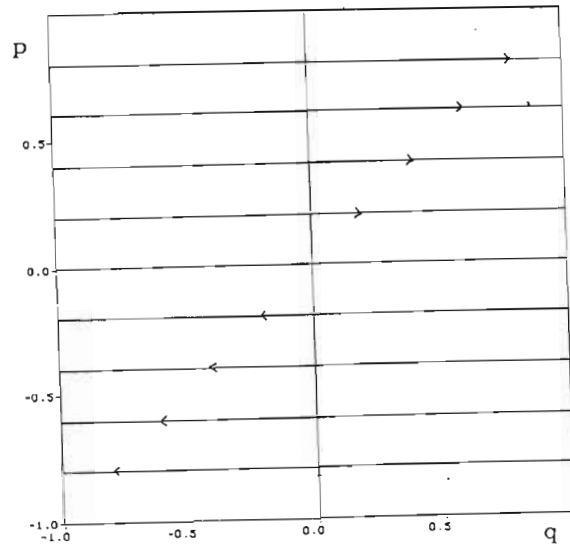


Figure 5: Phase portrait of a free particle (Example 1).

Example 2: Harmonic Oscillator

A one-dimensional particle moving in a quadratic potential has Hamiltonian

$$H(q, p) = \frac{1}{2}p^2 + \frac{1}{2}q^2, \quad (11)$$

and the equations of motion are thus

$$\frac{dq}{dt} = p, \quad \frac{dp}{dt} = -q, \quad (12)$$

Eq.(12) has solutions

$$\begin{aligned} p(t) &= q(0) \cos(t) + p(0) \sin(t), \\ q(t) &= -q(0) \sin(t) + p(0) \cos(t). \end{aligned} \quad (13)$$

This example shows the second topological type of ordered motion: *bounded uniform motion*. Motion takes place on concentric circles with the same angular speed (Figure 6).

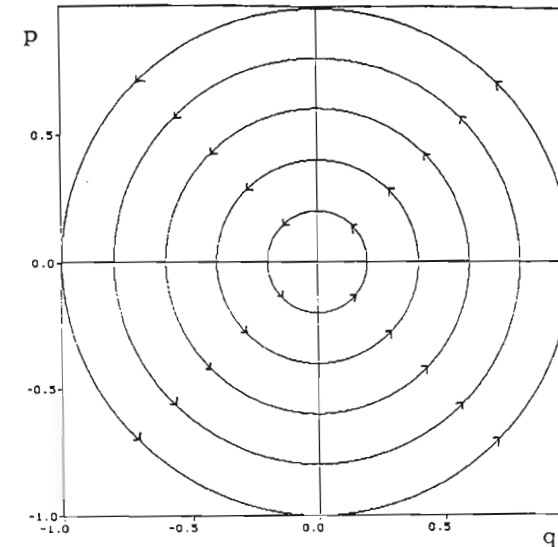


Figure 6: Phase portrait of the harmonic oscillator (Example 2).

Example 3: Pendulum

A system of particle motion subject to a periodic potential has Hamiltonian

$$H(q, p) = \frac{1}{2}p^2 + \cos(q), \quad (14)$$

and the equations of motion are thus

$$\frac{dq}{dt} = p, \quad \frac{dp}{dt} = \sin(q). \quad (15)$$

This example exhibits both bounded and unbounded motion in different regions of phase space (Figure 7). These regions are separated by a special curve called the separatrix. Which type of motion occurs will depend on the initial conditions.

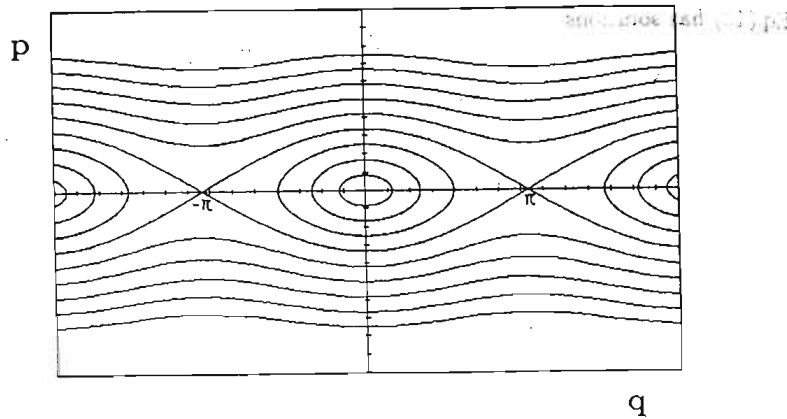


Figure 7: Phase portrait of the pendulum (Example 3).

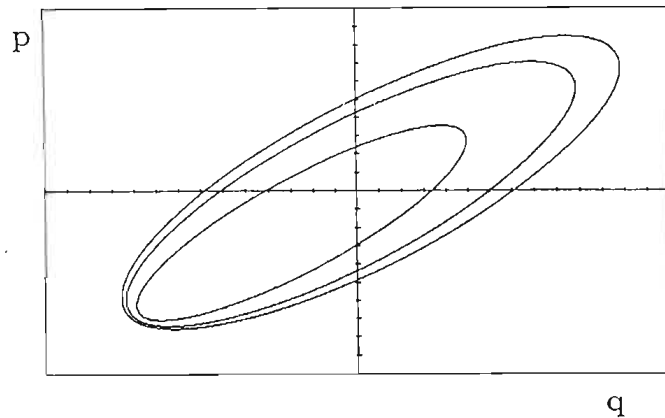


Figure 8: Phase portrait of the Kepler problem (Example 4). This is a projection of just three orbits; the phase space is four-dimensional.

Example 4: Kepler Problem The problem of two bodies moving in each others gravitational force field has Hamiltonian

$$H(q, p) = \frac{p_1^2}{2m_1} + \frac{p_2^2}{2m_2} - \frac{Gm_1m_2}{r_{12}}, \quad (16)$$

We do not reproduce the solutions to this problem here but they exhibit a direct product of free particle motion (the center of mass) and (stable) elliptic (Figure 8) or (unstable) hyperbolic motion.

2.2 Liouville-Arnold Theorem

We now give a formal definition of *integrability* as a prelude to the Liouville-Arnold theorem.

Definition: A system described by a Hamiltonian $H(\mathbf{q}, \mathbf{p})$, where $\mathbf{q}, \mathbf{p} \in \mathbb{R}^n$ is completely *integrable* if there are n (almost everywhere) functionally independent constants of the motion $F_i(\mathbf{q}, \mathbf{p})$, $i = 1, \dots, n$ such that all their Poisson brackets vanish:

$$\{F_k, F_l\} = 0 \quad k, l \in \mathbb{N}$$

The “almost everywhere” qualifier excludes exceptional points such as singular points of the vector field.

A system which has less than n constants of the motion (integrals) is called *nonintegrable*.

We now state an important theorem concerning integrable Hamiltonian systems.

Liouville-Arnold Theorem¹: Let L_c be a level set of the integrals F_i , $i = 1, \dots, n$, in an integrable system:

$$L_c := \{(\mathbf{q}, \mathbf{p}) \mid \mathbf{F}(\mathbf{q}, \mathbf{p}) = \mathbf{c}\}$$

and assume F_i are independent at each point of L_c . Then

- (1) There exists a differentiable coordinate transformation such that L_c becomes a “cylinder” $\mathbb{R}^k \times \mathbb{T}^{n-k}$ for some k .
- (2) Motion on such a cylinder is uniform: flow restricted to L_c is described by the linear equations

$$\dot{x}_1 = v_1(\mathbf{c})$$

$$\begin{aligned} & \vdots \\ \dot{x}_k &= v_k(\mathbf{c}) \\ \dot{\theta}_{k+1} &= \omega_{k+1}(\mathbf{c}) \\ & \vdots \\ \dot{\theta}_n &= \omega_n(\mathbf{c}) \end{aligned} \quad (17)$$

where $(x_1, \dots, x_k, \theta_{k+1}, \dots, \theta_n)$ are coordinates on the cylinder $\mathbf{R}^k \times \mathbf{T}^{n-k}$.

Several remarks are in order. Firstly for different level sets k may differ; also if the level set is compact (i.e. the motion is bounded) then motion takes place on an n -torus \mathbf{T}^n . In order to integrate a general (non-hamiltonian) system of $2n$ ODE's, we are required to find $2n$ integrals. The remarkable fact expressed by the Liouville-Arnold theorem is that for Hamiltonian systems only n integrals are required. We present a final example to illustrate the theorem.

Example 5: 3-Particle Toda Equation

This system describes three particles on a line with exponential interactions and has Hamiltonian

$$H(q, p) = \frac{1}{2}(p_1^2 + p_2^2 + p_3^2) + e^{q_1 - q_2} + e^{q_2 - q_3} \quad (18)$$

and the equations of motion can be expressed as a system of three coupled second order equations

$$\begin{aligned} \ddot{q}_1 &= -e^{q_1 - q_2} \\ \ddot{q}_2 &= e^{q_1 - q_2} - e^{q_2 - q_3} \\ \ddot{q}_3 &= e^{q_2 - q_3} \end{aligned} \quad (19)$$

The first and second integrals F_1 and F_2 are simply the Hamiltonian and the total momentum. The third integral F_3 does not have a simple interpretation and can be derived using a Lax representation (we omit the details here)

$$\begin{aligned} F_1 &:= H \\ F_2 &:= P = p_1 + p_2 + p_3 \\ F_3 &:= -p_1 p_2 p_3 + p_1 e^{q_2 - q_3} + p_3 e^{q_1 - q_2} \end{aligned} \quad (20)$$

It is easily verified that the mutual Poisson brackets (Eq.(2)) of the integrals vanish and thus that the system is completely integrable (this is also the case for the

previous examples). The Liouville-Arnold theorem can be applied here as we have three integrals and it tells us that motion takes place on "cylinders"

3. Chaos versus Order

In the last section we examined a number of examples of systems which are explicitly solvable and exhibit completely ordered motion. Most systems however are not explicitly solvable and we are thus led to the question of what sort of motion characterises such systems. What happens when an integrable system is perturbed in such a way that it is no longer integrable? The answer is that chaotic regions develop in phase space and that the measure occupied by the chaotic regions increases with increasing perturbation.

3.1 Fixed Points in Symplectic Maps

In the following discussion we restrict ourselves to two dimensional symplectic mappings for simplicity but all the notions discussed generalise to higher dimensional symplectic mappings unless otherwise stated. It is easy to see that the symplectic condition in two dimensions is equivalent to the condition that L preserves areas in phase space (in higher dimensions, being symplectic implies *much more* than just volume preservation).

Consider a general symplectic mapping $L: \mathbf{R}^2 \mapsto \mathbf{R}^2$. A *fixed* point of L is one which is invariant under L i.e. $L(\mathbf{x}) = \mathbf{x}$. One may also distinguish points which are invariant under n repeated applications of L , $L^n(\mathbf{x}) = \mathbf{x}$. These are called *higher order* fixed points or *periodic* points of L . We assume L has a fixed point at the origin (i.e. $L(0) = 0$) and expand L in a Taylor series about the origin

$$\begin{aligned} x' &= a_1 x + a_2 y + a_3 x^2 + a_4 xy + a_5 y^2 + \dots \\ y' &= b_1 x + b_2 y + b_3 x^2 + b_4 xy + b_5 y^2 + \dots \end{aligned} \quad (21)$$

where $a_i, b_i \in \mathbf{R}$ for $i \in \mathbf{N}$. We now calculate the Jacobian matrix of L and impose the area preserving condition

$$\det(J) = \det(dL) = \begin{vmatrix} \frac{\partial x'}{\partial x} & \frac{\partial x'}{\partial y} \\ \frac{\partial y'}{\partial x} & \frac{\partial y'}{\partial y} \end{vmatrix} = 1 \quad (22)$$

which implies in particular that the coefficients of the linear part of L satisfy $a_1 b_2 - b_1 a_2 = 1$. The eigenvalue equation is thus

$$\lambda^2 - (a_1 + b_2)\lambda + 1 = 0 \quad (23)$$

From Eq.(23) it can be deduced that generically there are two types of fixed points in 2D area preserving mappings. In the linear approximation of L (Eq.(21)) we examine each of these points in turn:

Elliptic Fixed Points

Elliptic fixed points have complex conjugate eigenvalues and thus the motion in the neighbourhood of such points occurs on (topological) circles. There is a coordinate transformation $(x, y) \mapsto (\hat{x}, \hat{y})$ such that

$$\begin{aligned} \hat{x}' &= \hat{x} \cos(2\pi\omega) - \hat{y} \sin(2\pi\omega) \\ \hat{y}' &= \hat{x} \sin(2\pi\omega) + \hat{y} \cos(2\pi\omega) \end{aligned} \quad (24)$$

(see Figure 9). The motion on each circle has the same angular speed ω . Elliptic fixed points are linearly stable.

Hyperbolic Fixed Points

Hyperbolic fixed points have real reciprocal eigenvalues, and motion in the neighbourhood of such points occurs on hyperbolae (Figure 10).

$$\begin{aligned} \hat{x}' &= \lambda \hat{x} \\ \hat{y}' &= \frac{1}{\lambda} \hat{y} \quad , \quad \lambda \in \mathbf{R}. \end{aligned} \quad (25)$$

Note in Figure 10 that there is an expanding and a contracting direction along the axes. These are known as the *stable and unstable manifolds* and in this (linear) case coincide with the direction of the eigenvectors. Hyperbolic fixed points are linearly unstable.

While the discussion has been restricted to fixed points of L it is not difficult to see that the fixed points of L^n generically are also elliptic or hyperbolic points. We have so far only considered elliptic and hyperbolic points in the linear approximation. We will now examine the behavior near these points when the nonlinear terms in L (Eq.(21)) are included. We will see that roughly speaking, elliptic points correspond to order, and hyperbolic points correspond to chaos.

3.2 Elliptic Fixed Points and the K.A.M. Theorem

Start from an integrable map L_0 with an elliptic fixed point at the origin which we write in polar coordinates (r, θ)

$$\begin{aligned} L_0 : \quad \theta' &= \theta + 2\pi\omega(r) \\ r' &= r \end{aligned} \quad (26)$$

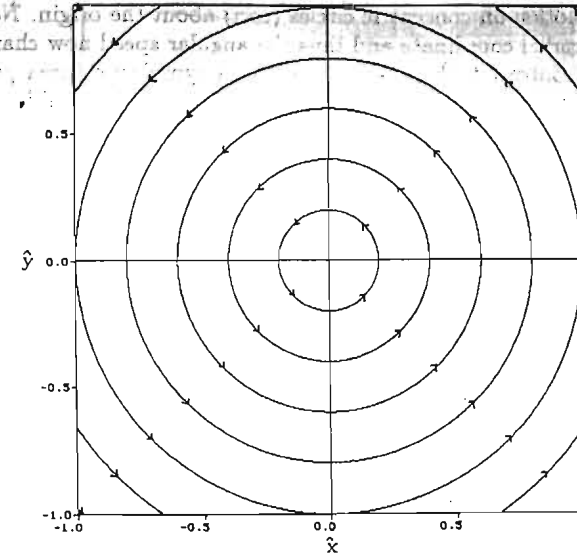


Figure 9: Motion in the neighbourhood of an elliptic fixed point.

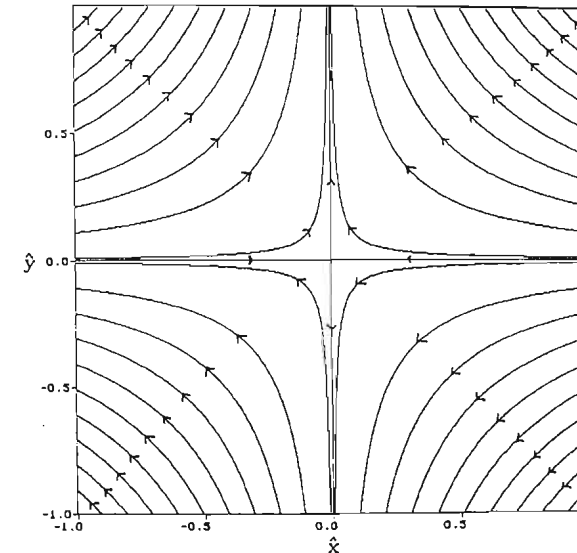


Figure 10: Motion in the neighbourhood of a hyperbolic fixed point.

Eq.(26) describes motion on concentric circles (tori) about the origin. Notice that θ' depends on the radial coordinate and thus the angular speed now changes from curve to curve (in contrast to Eq.(24)). Now add a symplectic (area preserving) perturbation term to Eq.(26) so that the system is no longer integrable,

$$\begin{aligned} L_\epsilon : \quad \theta' &= \theta + 2\pi\omega(r) + \epsilon f(\theta, r) \\ r' &= r + \epsilon g(\theta, r) \end{aligned} \quad (27)$$

We consider the fate of the tori in L_0 subject to ϵ perturbation terms. This is determined by the properties of the winding number ω . We consider two important cases:

- (i) $\omega(r_0)$ rational (i.e. resonant) \rightarrow the torus of radius r_0 breaks, leaving an even number of periodic orbits. Half are elliptic (representing "order"), half are hyperbolic (representing "chaos") (Poincaré-Birkhoff theorem),
- (ii) $\omega(r_0)$ is "sufficiently" irrational \rightarrow torus of radius r_0 persists. This is the content of the Kolmogorov-Arnold-Moser (K.A.M.) theorem which we give.

K.A.M. Theorem²: For L_ϵ there is a function $\gamma(\epsilon)$ such that there exists a smooth closed curve invariant under L_ϵ with winding number $\omega(r_0)$ provided

- (i) $|\omega(r_0) - p/q| \geq \gamma(\epsilon)|q|^{-2.5}, \forall p, q \in \mathbf{Z}/\{0\}$,
- (ii) $|\epsilon| \leq \epsilon_0(\omega(r_0))$.

The functional form of $\gamma(\epsilon)$ is not given by the theorem, but it tends to zero with ϵ . The theorem is of fundamental importance because it implies a certain *nonlinear* order near elliptic points.

Of importance is how many "sufficiently" irrational $\omega(r_0)$ are there? Take the rotation interval $0 \leq \omega \leq 1$ and shade in the excluded frequencies as the perturbation size ϵ increases from zero (Figure 11). This picture is slightly misleading because for *every* rational number there is an associated excluded region so we need to add all these regions up. We calculate an upper bound for the excluded fraction (shaded region of Figure 11) of frequencies:

$$\begin{aligned} \gamma(\epsilon)[1 + 2 \sum_{q=2}^{\infty} \frac{q-1}{q^{2.5}}] &= \gamma(\epsilon)[1 + 2 \sum_{q=1}^{\infty} (q^{-1.5}) - 2 \sum_{q=1}^{\infty} (q^{-2.5})] \\ &= \gamma(\epsilon) \cdot 3.54176... \end{aligned} \quad (28)$$

So the excluded fraction of frequencies goes to zero with ϵ . It follows that for a sufficiently small ϵ a large measure of tori persist.

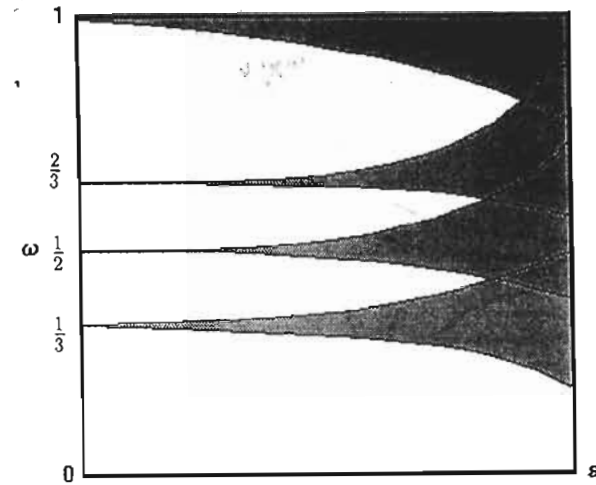


Figure 11: Schematic diagram of the rotation number (ω) versus perturbation strength (ϵ). Shaded regions denote the excluded frequencies.

3.3 Hyperbolic Fixed Points and Homoclinic Horseshoes

Recall the linearised neighbourhood of a hyperbolic fixed point described earlier for the mapping L . The stable and unstable manifolds of a nonlinear integrable map (M_s and M_u) closely resemble those of a linear map within a sufficiently small neighbourhood of a hyperbolic fixed point, and are in fact tangent to the linearised curves at the fixed point (Figure 12).

What happens when you follow M_s and M_u away from H ? In an integrable map there are three possibilities :

1. M_s and M_u go off to infinity,
2. M_s meets M_u of the *same* fixed point and coincides with it exactly,
3. M_s meets M_u of *another* fixed point and coincides with it exactly.

We illustrate the three possibilities schematically in Figure 13. In the second case the loop formed by the exact coincidence of M_s and M_u is called a *homoclinic* orbit. In the third case the connecting curve is called a *heteroclinic* orbit. Note that neither M_s or M_u can intersect itself.

We illustrate these ideas with a real example in Figure 1 which is in fact a phase plot of the following two-dimensional integrable map L_0 , which has a hyperbolic fixed point at the origin:

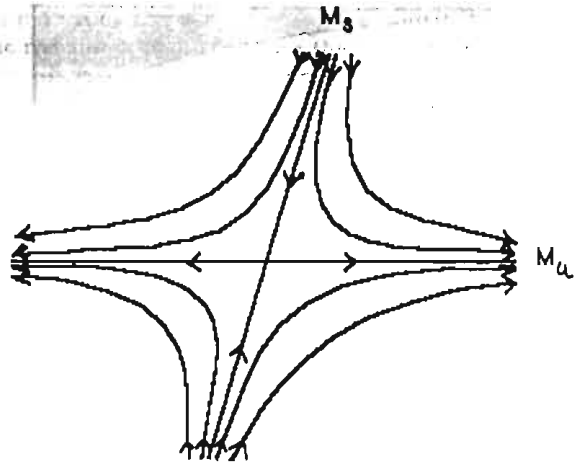


Figure 12: The neighbourhood of a hyperbolic fixed point in a nonlinear integrable mapping illustrating the stable and unstable manifolds (W_s and W_u resp.).

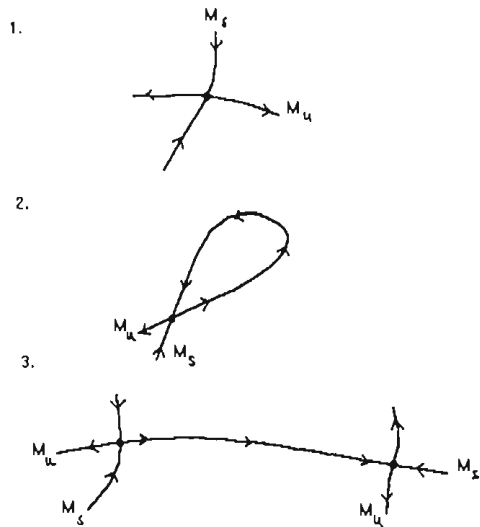


Figure 13: The three possible configurations of M_s and M_u in an integrable map.

and the unperturbed system $L_0 : \begin{cases} x' = y \\ y' = -x + \frac{2ky}{1+y^2} \end{cases}$ (29)

where k is a free parameter.

Now add a symplectic perturbation term to Eq.(29) so that the system is no longer integrable,

$$L_\epsilon : \begin{cases} x' = y + \epsilon f(x, y) \\ y' = -x + \frac{2ky}{1+y^2} + \epsilon g(x, y) \end{cases} \quad (30)$$

We now consider the fate of the stable and unstable manifolds in L_0 subject to ϵ perturbation terms. The exact coincidence of M_u and M_s is fragile and does not persist. What often happens is that M_u and M_s that coincided in the integrable case now intersect at a point (called a *homoclinic point*). If there is one intersection there are infinitely many. Actually between any two intersections there are infinitely many more intersections³. Since L_0 is area-preserving the areas enclosed by W_s and W_u must be the same, resulting in extreme convolutions of the manifolds as they approach the fixed point (Figure 14). This leads to the formation of a *homoclinic tangle*.

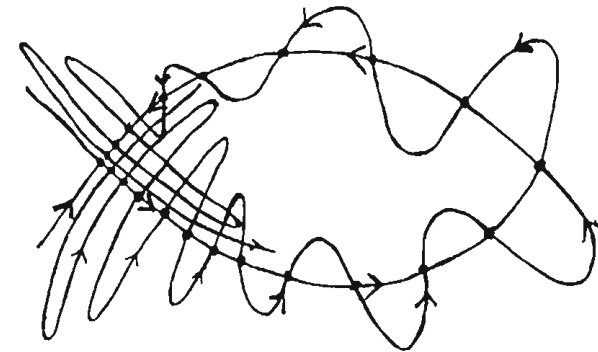


Figure 14: A homoclinic tangle in the neighbourhood of a hyperbolic fixed point.

It can be shown that in the neighbourhood of such a homoclinic tangle there exists an invariant set Λ such that the dynamics on Λ is equivalent to that on a Smale horseshoe (a prototypical model for chaos) and further that

1. There is *sensitivity to initial conditions* on Λ .
2. Periodic orbits are dense in Λ .
3. There is a dense orbit in Λ .

These three properties define *chaos*. In Devaney (1989) there is a topological transitivity condition rather than property 3 above⁴, but note that the existence of a dense orbit implies topological transitivity. Actually properties 2 and 3 can be shown to imply property 1⁵. Note that property 1 is *not* invariant under coordinate transformations (symplectic or otherwise) but properties 2 and 3 are coordinate invariant.

3.4 Putting it all Together

We now know what happens to stable and unstable fixed points in integrable systems under small nonintegrable perturbations. It should be noted that the K.A.M. theorem stated above is global in nature. We must next treat the *local* K.A.M. theorem. This says that near a *generic* elliptic fixed point of a nonintegrable map an analogous result holds where ϵ now represents the distance from the fixed point. The Poincaré-Birkhoff theorem also holds near a generic elliptic fixed point. So we get all the phenomena that operate at the "global" level, occurring on successively smaller scales. This incredibly complicated state of affairs is indicated schematically in Figure 15.

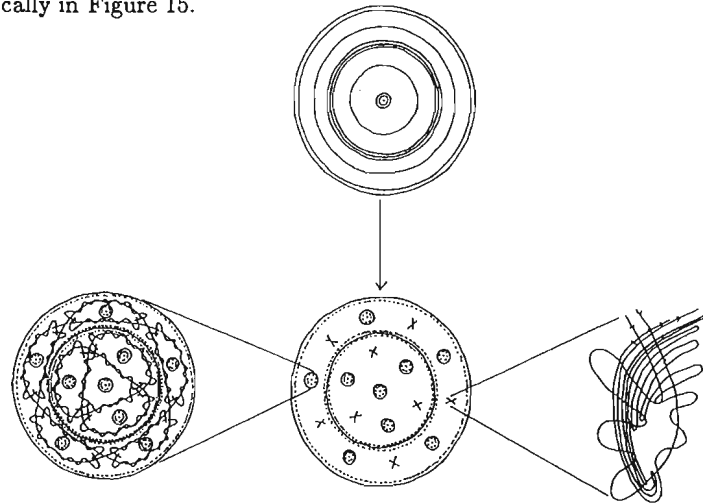


Figure 15: Schematic representation of the repeated application of the K.A.M. and Poincaré-Birkhoff theorems show order and chaos on all scales.

An example of a perturbation of the integrable map Eq.(29) actually exhibiting all these phenomena is given by

$$L_\epsilon: \begin{aligned} x' &= y \\ y' &= -x + \frac{2ky}{1+y^2} + \epsilon y^2 \end{aligned} \quad (31)$$

The phase plots of this map are given in Figures 16(a) and 16(b).

4. Measuring Chaos Numerically

4.1 Lyapunov Exponents

As mentioned above, one of the hallmarks of chaos is sensitivity to initial conditions. It is desirable to construct some practical measure of chaos so that given a particular orbit in phase space, one can make a statement concerning the behavior of the orbit. How is sensitivity measured? If a region is chaotic, nearby points separate exponentially fast on average. This is what we mean by "sensitivity to initial conditions". The exponential growth rates are called *Lyapunov exponents**.

Lyapunov Exponents in 1-D

Let x and y be two nearby initial points

$$|L^n(x) - L^n(y)| \simeq |x - y| \exp(\lambda n) \quad (32)$$

We rearrange Eq.(32) to give

$$\frac{1}{n} \ln \left(\frac{|L^n(x) - L^n(y)|}{|x - y|} \right) \rightarrow \lambda \quad \text{as } n \rightarrow \infty \quad (33)$$

In a bounded region x and y must be very close. So we impose the limit as $|x - y| \rightarrow 0$ and the resulting quantity defines the Lyapunov exponent (λ) of the orbit through the point y

$$\lambda := \lim_{n \rightarrow \infty} \frac{1}{n} \lim_{|x - y| \rightarrow 0} \ln \left(\frac{|L^n(x) - L^n(y)|}{|x - y|} \right) \quad (34)$$

The bracketed term is simply the Newton quotient so that in the limit $|x - y| \rightarrow 0$ we have the following approximation

* Note that the definition of Lyapunov exponents is valid also for non-Hamiltonian systems.

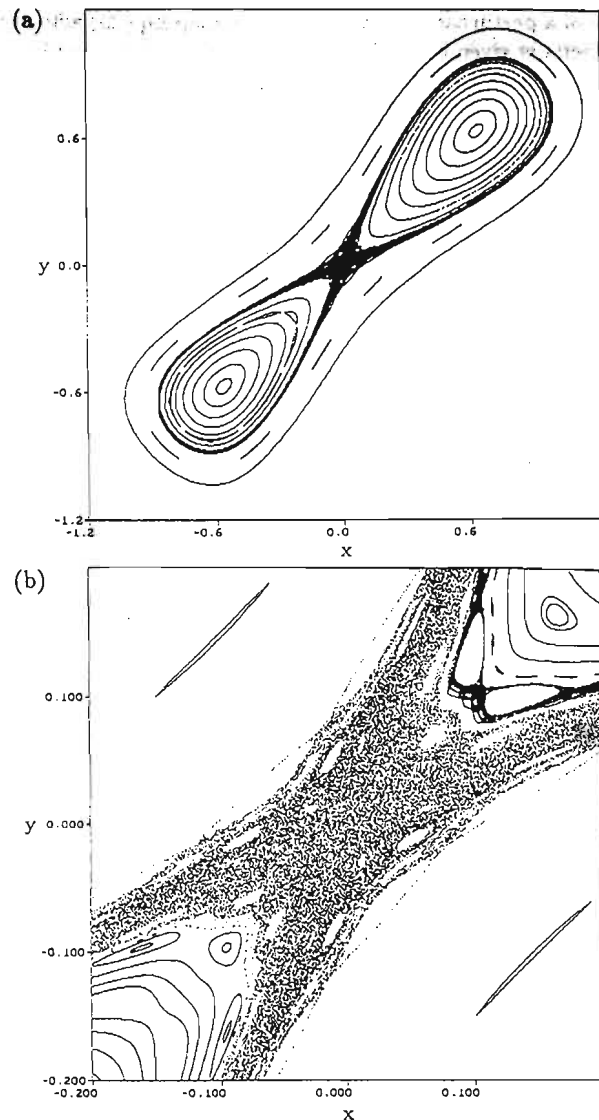


Figure 16: Plots of the perturbed mapping Eq.(31) with $\epsilon = 0.09$ and $k = 1.36$; (a) the same set of initial conditions as for Figure 1 and (b) an enlargement of (a) with a more finely spaced set of initial conditions in the vicinity of the hyperbolic fixed point at the origin. The dense chaotic region is generated by a single initial condition.

... necessary to calculate the Lyapunov exponent under certain mathematical conditions
 ... low exponents ...

$$L^n(x) - L^n(y) \approx \frac{DL^n(y)}{Dy} \cdot (x - y) \quad (35)$$

Example: A special case of the logistic map $L: \mathbf{R} \rightarrow \mathbf{R}$ is

$$L: y' = 4y(1 - y) \quad (36)$$

and its explicit solution for $y \in [0, 1]$ is given by

$$L^n(y) = \frac{1}{2} - \frac{1}{2} \cos[2^n \cdot \arccos(1 - 2y)] \quad (37)$$

Calculate the Lyapunov exponent using Eq.(34)

$$\begin{aligned} \lambda &= \lim_{n \rightarrow \infty} \frac{1}{n} \ln \left(\frac{\left| \frac{DL^n(y)}{Dy} \right| \cdot (x - y)}{|x - y|} \right) \\ &= \lim_{n \rightarrow \infty} \frac{1}{n} \ln \left| \frac{DL^n(y)}{Dy} \right| \\ &= \lim_{n \rightarrow \infty} \frac{1}{n} \ln \left| \frac{D\left(\frac{1}{2} \cos[2^n \cdot \arccos(1 - 2y)]\right)}{Dy} \right| \\ &= \lim_{n \rightarrow \infty} \frac{1}{n} \ln \left| 2^{n-2} \cdot \frac{\sin[2^n \cdot \arccos(1 - 2y)]}{\sqrt{y - y^2}} \right| \\ &= \ln 2 \quad (38) \end{aligned}$$

It is of course extremely unusual that the solution of a mapping can be given in closed form, and therefore usually we must rely on numerical methods in the calculation of Lyapunov exponents.

Lyapunov Exponents in m-D

Lyapunov exponents can be extended to m-dimensions ($m > 1$): we have a spectrum of Lyapunov exponents (Figure 17):

$$\lambda_1 \geq \lambda_2 \geq \dots \geq \lambda_m \quad (39)$$

Claim - We can still calculate λ_1 as follows

$$\lambda_1 = \lim_{n \rightarrow \infty} \frac{1}{n} \lim_{|x-y| \rightarrow 0} \ln \left(\frac{|L^n(x) - L^n(y)|}{|x - y|} \right) \quad (40)$$

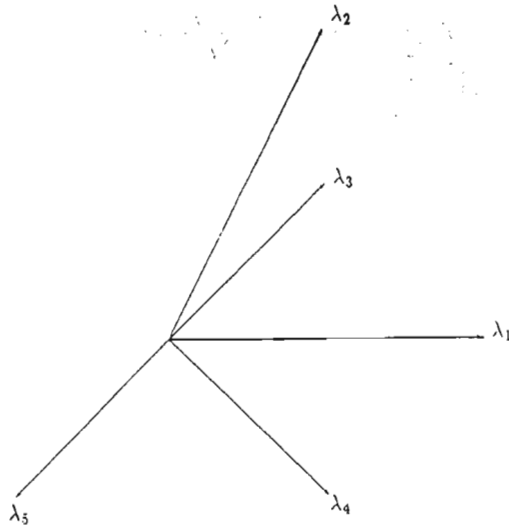


Figure 17: Schematic representation of the averaged eigenvectors ("Lyapunov vectors") at a point along a trajectory. The lengths of these vectors represent the Lyapunov exponents, λ_i .

Proof: As $|x - y| \rightarrow 0$ we have

$$L^n(x) - L^n(y) \simeq \frac{DL^n(y)}{Dy} \cdot (x - y)$$

As $n \rightarrow \infty$, $\frac{DL^n(y)}{Dy}$ has eigenvalues $e^{\lambda_1 n}, e^{\lambda_2 n}$ on average. Expand the difference $x - y$ in terms of the basis of eigenvectors e_1, e_2, \dots

$$x - y = \sum_{i=1}^m \alpha_i e_i$$

Eq.(40) becomes

$$\lim_{n \rightarrow \infty} \frac{1}{n} \lim_{\alpha_i \rightarrow 0} \ln \left(\frac{|\sum_{i=1}^m \alpha_i e^{\lambda_i n} e_i|}{|\sum_{i=1}^m \alpha_i e_i|} \right) = \lim_{n \rightarrow \infty} \frac{1}{n} \lim_{\alpha_i \rightarrow 0} \ln \left(\frac{\alpha_1 e^{\lambda_1 n}}{|\sum_{i=1}^m \alpha_i e_i|} \right) = \lambda_1$$

It is also possible to calculate the other Lyapunov exponents $\lambda_2, \lambda_3, \dots, \lambda_m$ through repeated orthonormalisation of the eigenvectors⁶. In Hamiltonian systems the Lyapunov exponents occur in pairs ($\lambda_i = -\lambda_{m-i+1}$, $m = 2n$, and $1 \leq i \leq n$) and it is

only necessary to calculate $\frac{m}{2}$ exponents. Under certain mathematical conditions Lyapunov exponents are constant for all orbits in a given chaotic region⁷.

Example 1: The Restricted Three-body problem.

We have seen how chaos is often created by a (nonintegrable) perturbation of an integrable system. The restricted three-body problem is a nice illustration of this idea. We can start with the integrable two-body problem (with one large body and one small body) and then introduce a second large body, initially at large distance so that the interaction is weak. By moving the the second large body closer to the pair we create a competition between the forces of the two larger bodies resulting in the motion of the smaller body becoming chaotic (Figure 18).

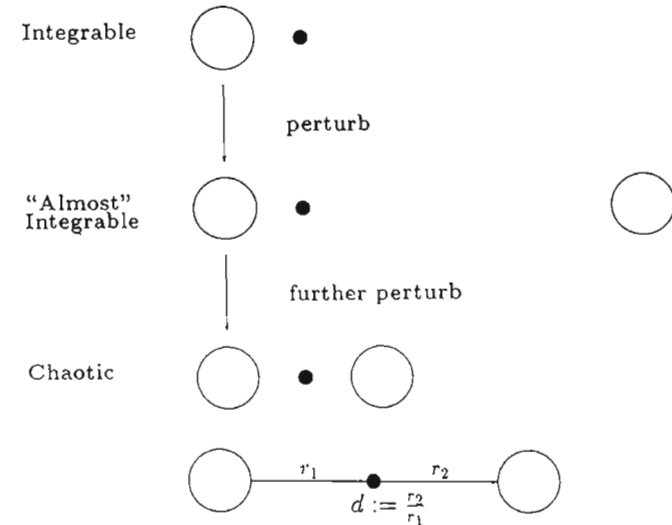


Figure 18: Schematic diagram of the restricted three-body problem.

We present some results of the work of Gonczi and Froeschle (1981) who studied the development of stochasticity in the planar restricted three-body problem via Lyapunov exponents⁸. They observe that if there exist p (approximate) integrals in a region where an orbit lies, then $2p$ Lyapunov exponents vanish. This behavior is indicated in Figure 19 which clearly illustrates a transition from an ordered region ($d \leq 0.25$) where there are three isolating integrals and all three exponents are small, to a chaotic region where two of the exponents are large in relation to the third indicating the disappearance of two integrals. This problem has three degrees-of-freedom so only three Lyapunov exponents are required.

Example 2: Non-integrable area preserving mapping L_c .

The Lyapunov exponent of the mapping L_c (Eq.(31)) is plotted in Figure 20. We plot the Lyapunov exponent of 13 orbits as a function of their initial conditions occurring along the -0.12 to 0.0 portion of the line $y = x$ (see Figure 16(b)). Again one observes a transition from ordered to chaotic behavior at $x \approx -0.07$ as the hyperbolic fixed point (at $x = y = 0$) is approached.

4.2 Symplectic Integration

If we want to perform an accurate numerical integration of a Hamiltonian system of ODE's (to find out whether it has sensitive dependence on initial conditions, for instance), it is essential to preserve the symplectic structure of the equations. If we do not do this, all the above theorems lose their validity, and spurious dissipation effects arise. The question thus arises whether it is possible to approximate Hamiltonian flows by symplectic maps? Recalling Hamilton's equation (Eq.(4)) it is convenient to rewrite this as

$$\frac{dz}{dt} = \left[\omega \cdot \frac{\partial H}{\partial z} \frac{\partial}{\partial z} \right] z \quad (41)$$

Since H has no explicit time-dependence, Eq.(41) has the formal solution

$$z(t) = e^{tA} z(0) \quad (42)$$

where

$$A := \omega \cdot \frac{\partial H}{\partial z(0)} \frac{\partial}{\partial z(0)} \quad (43)$$

The problem now becomes how to approximate e^{tA} . We could use a series expansion of the exponential operator to rewrite Eq.(42) as

$$z(t) = z(0) + tAz(0) + \frac{t^2}{2} A^2 z(0) + \dots \quad (44)$$

There is however a problem with this series solution in that its truncation invariably yields a map $z(0) \mapsto z(t)$ which is not symplectic. To remedy this, assume that we can decompose the Hamiltonian H

(24)

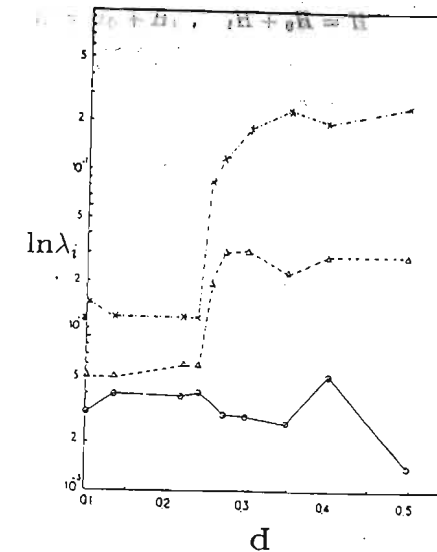


Figure 19: Lyapunov exponents λ_i for $i = 1, \dots, 3$ are plotted against the distance ratio d (from Gonczi and Froeschle (1981)).

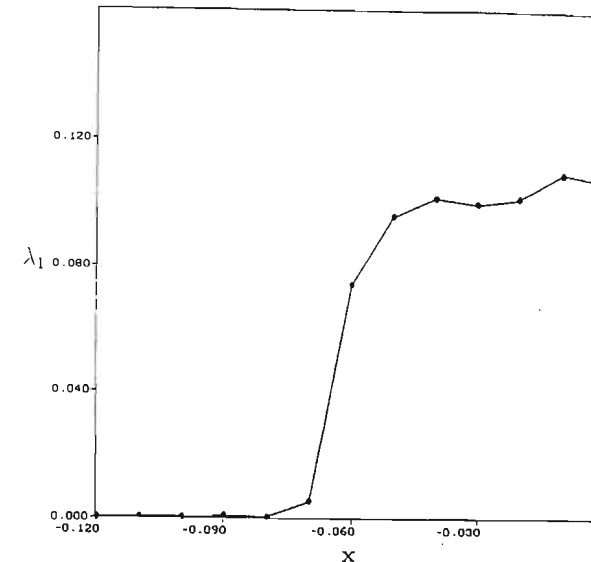


Figure 20: Lyapunov exponent λ_1 versus distance x . A transition occurs at $x \approx -0.07$.

$$H = H_0 + H_1 \quad , \quad (45)$$

and thus

$$A = A_0 + A_1 \quad , \quad (46)$$

where A_0 and A_1 are such that we do know e^{tA_0} and e^{tA_1} . Claim - For small time (integration) step τ the product $e^{\tau A_0} e^{\tau A_1}$ is a symplectic approximation to $e^{\tau A}$.

Proof:

1. We first show that the exponential product is an approximation to $e^{\tau A}$.

$$\begin{aligned} e^{\tau A_0} e^{\tau A_1} &= e^{\tau A_0 + \tau A_1 + \frac{1}{2}\tau^2[A_0, A_1] + \dots} \\ &= e^{\tau A} + O(\tau^2) \quad , \end{aligned}$$

where $[,]$ denotes the Lie bracket.

2. Secondly we show that the approximation is symplectic. By assumption $e^{\tau A_0}$ and $e^{\tau A_1}$ are symplectic, by the group property of symplectic maps, so is their product.

Several comments are in order. The approximation improves for $H_0 \gg H_1$ (one can think of H_1 as a small perturbation term in the Hamiltonian). The method described is a very crude example of an integration scheme which preserves the symplectic structure. There exist very sophisticated methods of generating higher order symplectic integrators^{9,10}.

4.9 Is the Solar System Stable?

We now present an application of the techniques discussed in this section. They are applied to a very famous problem in celestial mechanics which attempts to determine the stability of the configuration of planets in the solar system¹¹. It has long been known that there exist initial conditions leading to chaotic orbits of the n-body system. What interests us here is the question whether the *actual* orbit of the solar system (i.e. that's us!) is chaotic. As a starting point the Hamiltonian for a classical system of n-bodies in a gravitational force field is

$$H = \sum_{i=0}^{n-1} \frac{p_i^2}{2m_i} - \sum_{i \neq j} \frac{Gm_i m_j}{r_{ij}} \quad , \quad (47)$$

where r_{ij} is the Euclidean distance between the bodies i and j . To obtain an accurate symplectic integrator Eq.(47) can be written as the sum of n decoupled Kepler Hamiltonians, plus a (small) interaction Hamiltonian. Introducing Jacobi variables H is rewritten as

$$\begin{aligned} H &= H_0 + H_1 \\ H_0 &= \sum_{i=1}^{n-1} \left(\frac{p_i^2}{2m'_i} - \frac{Gm_i m_0}{r'_{i1}} \right) \\ H_1 &= \sum_{i=1}^{n-1} Gm_i m_0 \left(\frac{1}{r'_i} - \frac{1}{r_{i0}} \right) - \sum_{0 \leq i < j} \frac{Gm_i m_j}{r_{ij}} \quad , \quad (48) \end{aligned}$$

where

$$\begin{aligned} r'_i &:= \left| \mathbf{r}_i - \frac{\sum_{j=0}^i m_j \mathbf{r}_j}{\sum_{j=0}^{i-1} m_j} \right| \quad , \quad r_{ij} := |\mathbf{r}_i - \mathbf{r}_j| \quad 0 \geq i \geq j \\ m'_i &:= \frac{m_i \sum_{j=0}^{i-1} m_j}{\sum_{j=0}^i m_j} \quad 0 \leq i < n, \quad m'_n = \sum_{i=0}^{n-1} m_i \quad . \end{aligned}$$

We now present the work Sussman and Wisdom (1990) who have performed extensive numerical simulations of the solar system using symplectic integrators¹². They choose a time step $\tau = 7.2$ days and integrate the system forward in time for 36 billion days ≈ 100 million years. Initial condition differed by 1 millimeter in the x coordinate of Pluto. The result is indicated in Figure 21. There is a clear piecewise linear increase in the logarithm of the separation (d_s) of the two orbits which indicates sensitive dependence on initial conditions.

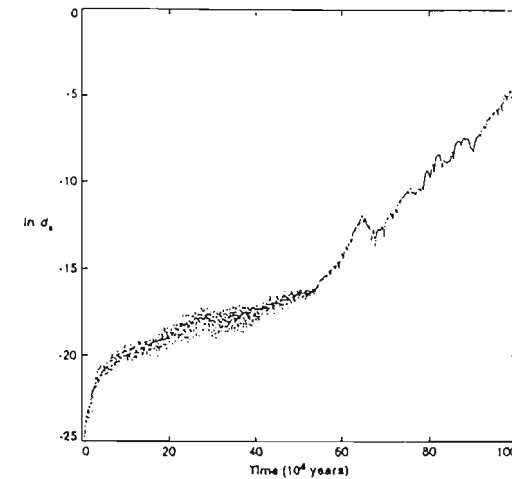


Figure 21: Logarithm of the distance between the two orbits $\ln d_s$ versus time indicating sensitivity to initial conditions (from Sussman & Wisdom (1990)).

5. Conclusions and Outlook

The above study is not the only indication of chaos in the solar system. If the planets are not treated as point particles, but as rotating rigid bodies, it is found that their axis of rotation moves chaotically. Studies are also underway to find the mechanisms explaining the discovered sensitivity to initial conditions.

Surveying the field of chaotic dynamical systems in general, I believe it is fair to say that we are starting to obtain results for systems that are relevant to applications in the natural sciences. Many areas are beginning to show future promise. To name just a few. Studies in the control of chaos show ways in which chaos can be used to our advantage, instead of as a nuisance¹³ to be avoided. Another area where a lot of research is going on is Quantum Chaos¹⁴. In quantum theory there is a smallest length scale (\hbar) which is not present in classical systems. The theory of Quantum Chaos studies the implications this has for the possible occurrence of chaos in quantum systems.

Finally, initial steps have been set on the path to understanding chaos and turbulent behavior in systems with an infinite number of degrees of freedom. In the conservative case¹⁵ this has relevance for the foundations of statistical mechanics, in the dissipative¹⁶ case there beckons the still not well understood problem of hydrodynamic turbulence.

Acknowledgements

The author acknowledges the support of the Australian Research Council.

References

1. V.I.Arno'd, *Mathematical Methods of Classical Mechanics* (2nd Ed.), Springer-Verlag, 1989.
2. M.Tabor, *Chaos and Integrability in Nonlinear Dynamics - An Introduction*, Wiley, 1989.
3. E.A.Jackson, *Perspectives in Nonlinear Dynamics* Vol. 1, C.U.P., 1990.
4. R.L.Devaney, *An Introduction to Chaotic Dynamical Systems* (2nd Ed.), Addison-Wesley, 1989.
5. J.Banks, J.Brooks, G.Cairns, G.Davis and P.Stacey, 'On Devaney's definition of chaos', *Amer.Math.Mon.* **99** (1992) 332.
6. G.Benettin, L.Galgani, A.Giorgilli and J-M.Strelcyn, 'Lyapunov characteristic exponents for smooth dynamical systems; a method for computing all of them', *Meccanica* **15** (1980) 1 Part 1: Theory, 9; Part 2: Numerical application, 21.
7. V.I.Oseledec, 'A multiplicative ergodic theorem. Ljapunov characteristic numbers for dynamical systems', *Trans.Moscow Math.Soc.* **19** (1968) 197.

8. R.Gonczy and C.Froeschle, 'The Lyapunov characteristic exponents as indicators of stochasticity in the restricted three-body problem', *Celest.Mech.* **25** (1981) 2271.
9. H.Yoshida, 'Construction of higher order symplectic integrators', *Phys.Lett.A* **150** (1990) 262.
10. J.M.Sanz-Serna, 'Symplectic integrators for Hamiltonian problems: an overview', *Acta Numerica* **1** (1991) 243.
11. J.Moser, 'Is the solar system stable?', *Math.Intelligencer* **1** (1978) 65.
12. G.J.Sussman and J.Wisdom, 'Numerical evidence that the motion of Pluto is chaotic', *Science* **241** (1990) 433.
13. T.Shinbrot, W.Ditto, C.Grebogi, E.Ott, M.Spano and J.A.Yorke, 'Using the sensitive dependence of chaos (the "butterfly effect") to direct trajectories in an experimental chaotic system', *Phys.Rev.Lett.* **68** 2863.
14. M.C.Gutzwiller, *Chaos in Classical and Quantum Systems*, Springer-Verlag, 1990.
15. C.E.Wayne, 'The KAM theory of systems with short range interactions', *Commun.Math.Phys.* **96** (1984) Part I 311, Part II 330.
16. R.Temam, *Infinite-Dimensional Dynamical Systems in Mechanics and Physics* Springer-Verlag, Applied Mathematical Sciences Vol. 68, 1988.

Recommended Reading

Semipopular:

J.Gleick, *Chaos*, Macdonald & Co., 1987.

I.Peterson, *Newton's Clock: Chaos in the Solar System*, W.H.Freeman, 1993.

Books written by Physicists:

E.Ott, *Chaos in Dynamical Systems*, C.U.P., 1993.

E.A.Jackson, *Perspectives in Nonlinear Dynamics*, Vol. 1 & 2 C.U.P., 1990.

Books written by Mathematicians:

J.Banks and V.Dragan, *Chaos, A Mathematical Introduction*, LaTrobe University, 1993.

R.L.Devaney, *An Introduction to Chaotic Dynamical Systems* (2nd Ed.), Addison-Wesley, 1989.

Related interest :

M.Mitchell Waldrop, *Complexity*, Penguin, 1992.